USGS
science for a changing world

Elastic Properties of Overpressured and Unconsolidated Sediments

By Myung W. Lee

U.S. Geological Survey Bulletin 2214

Version 1.0 2003

U.S. Department of the Interior
U.S. Geological Survey

Elastic Properties of Overpressured and Unconsolidated Sediments

By Myung W. Lee

U.S. Geological Survey Bulletin 2214

U.S. Department of the Interior
U.S. Geological Survey

U.S. Department of the Interior
Gale A. Norton, Secretary

U.S. Geological Survey
Charles G. Groat, Director

Posted online September 2003, version 1.0

For more information about the USGS and its products:
Telephone: 1-888-ASK-USGS
World Wide Web: http://www.usgs.gov/

This publication is only available online at:
http://geology.cr.usgs.gov/pub/bulletins/b2214/

Contents

Figures

Table

Elastic Properties of Overpressured and Unconsolidated Sediments

By Myung W. Lee

Abstract

Differential pressure affects elastic velocities and Poisson's ratio of sediments in such a way that velocities increase as differential pressure increases. Overpressured zones in sediments can be detected by observing an increase in Poisson's ratio with a corresponding drop in elastic velocities. In highly overpressured sands, such as shallow water flow sands, the *P*- to *S*-wave velocity ratio (V_p/V_s) is very high, on the order of 10 or higher, due to the unconsolidated and uncemented nature of sediments. In order to predict elastic characteristics of highly overpressured sands, Biot-Gassmann theory by Lee (BGTL) is used with a variable exponent *n* that depends on differential pressure and the degree of consolidation/compaction. The exponent *n* decreases as differential pressure and the degree of consolidation increases, and, as *n* decreases, velocity increases and V_p/V_s decreases. The predicted velocity ratio by BGTL agrees well with the measured velocity ratio at low differential pressure for unconsolidated sediments.

Introduction

Knowledge of fluid pressure in the pore spaces of sedimentary rocks is important for the successful exploration and production of hydrocarbons. High pore pressure, commonly associated with shallow and unconsolidated sediments, presents a significant hazard during drilling and completion of offshore wells. Therefore, predicting overpressured intervals before drilling not only mitigates drilling hazard but also minimizes drilling cost.

One exploration problem in deep water is encountering shallow-water-flow (SWF) sands (Sayers and others, 2001; Bruce and others, 2002; Mallick and others, 2002; Ostermeier and others, 2002). SWF sands are overpressured and unconsolidated (Huffman and Castagna, 2001; Bruce and others, 2002). During drilling, SWF sand may flow into the well if their pore pressures are not balanced by mud weight, causing large and long-lasting uncontrolled flows, well damage, foundation failure, damaged casing, reentry, and control problems (Ostermeier and others, 2002). Seismic methods have been used to predict these important overpressured intervals (Huffman and Castagna, 2001; Dutta, 2002; Mallick and others, 2002; Sayers and others, 2002).

Physical properties of SWF sands differ from most reservoir and seal rocks for petroleum. These materials exist near transition zones between rock and sediment (Huffman and Castagna, 2001). SWF sands usually have high porosities and very low differential pressure or high pore pressure; they are unconsolidated and uncemented. Therefore, interval velocities (*P*-wave and *S*-wave velocity) of SWF sands are low compared to adjacent normally pressured sands, and the decrease of velocity is related to the amount of overpressure (Huffman and Castagna, 2001; Prasad, 2002). With increasing pore pressure, SWF sands lose cohesion, causing V_s to drop faster than V_p. This causes V_p/V_s to increase rapidly. A typical V_p/V_s ratio of SWF sand is on the order of 10 or higher (Mallick and others, 2002).

Sayers and others (2002) predicted pore pressure using reflection tomography and four-component (4-C) seismic data. Reflection tomography gives higher spatial resolution for interval velocities, and 4-C data may help to reduce the ambiguity between variations in pore pressure and variations in lithology and fluid content. Dutta (2002) used prestack inversion of large-offset *P*-wave data and rock models to predict deep water geohazards or overpressure. Both approaches utilize the reduction of *P*- and *S*-wave velocities and the high V_p/V_s ratio for overpressured intervals. Because large changes in Poisson's ratio of SWF sands also result in significant changes in the amplitude versus offset (AVO) response, high-resolution AVO and inversion methods should be able to resolve changes in pressure (Huffman and Castagna, 2001).

One key element in predicting overpressure is the relationship between differential pressure and V_p/V_s. Empirical relationships between differential pressure, V_p/V_s, and velocities with respect to differential pressure are presented by Huffman and Castagna (2002) and Prasad (2002). Zimmer and others (2002) investigated pressure and porosity influence on V_p/V_s in unconsolidated sands using glass bead samples. In this paper, elastic velocities of overpressured unconsolidated sediments are predicted by the Biot-Gassmann theory by Lee or BGTL (Lee, 2002, 2003). Velocities or velocity ratios with respect to differential pressure are incorporated by using a variable exponent *n* as a function of differential pressure and consolidation/compaction. Predicted velocities or velocity

ratios by BGTL agree well with measured data complied by Prasad (2002) and Huffman and Castagna (2001).

Theory

Based on an assumption that the velocity ratio (V_p/V_s) depends on porosity, Lee (2002, 2003) derived the following elastic moduli for water-saturated sediments:

$$k = k_{ma}(1-\beta) + \beta^2 M \tag{1}$$

$$\mu = \frac{\mu_{ma} k_{ma}(1-\beta)G^2(1-\phi)^{2n} + \mu_{ma}\beta^2 M G^2(1-\phi)^{2n}}{k_{ma} + 4\mu_{ma}\left[1 - G^2(1-\phi)^{2n}\right]/3} \tag{2}$$

with

$$\frac{1}{M} = \frac{(\beta-\phi)}{k_{ma}} + \frac{\phi}{k_{fl}}$$

where

k and μ are bulk and shear moduli of water-saturated sediments, respectively,

k_{ma} , μ_{ma}, and k_{fl} are bulk and shear moduli of matrix material and bulk modulus of fluid, respectively,

β and ϕ are the Biot coefficient and porosity, respectively, and

n and G are parameters that depend on the degree of consolidation/compaction, differential pressure, and clay content.

Elastic velocities, V_p for *P*-wave and V_s for *S*-wave velocities, of water-saturated sediments can be computed from the elastic moduli by the following formulas:

$$V_p \quad \sqrt{\frac{k + 4\,\mu/3}{\rho}} \qquad \text{and} \qquad V_s = \sqrt{\frac{\mu}{\rho}} \tag{3}$$

where

ρ is density of the formation.

The formation density is given by

$$\rho = (1-\phi)\,\rho_{ma} + \phi\rho_{fl} \tag{4}$$

where

ϕ, ρ_{ma} and ρ_{fl} are porosity, matrix density , and pore fluid density, respectively.

Lee (2003) referred to the above method of computing shear modulus as BGTL , Biot-Gassmann theory by Lee, to differentiate from the classical Biot-Gassmann theory (BGT) (Biot, 1956; Gassmann, 1951), which computes shear modulus by $\mu = \mu_{ma}(1 - \beta)$. Note that, as indicated in Lee (2003), there is no difference between BGT and BGTL for a dry or gas-saturated rock.

BGTL Parameters

Biot Coefficient

Within the poroelastic framework, skeleton or frame moduli, k and μ, are undetermined and must be specified a priori. The moduli of a dry frame are related to the moduli of matrix material through the Biot coefficient, β. Usually, β depends on differential pressure as well as porosity, but the following Biot coefficient as a function of porosity for unconsolidated sediments (Lee, 2002) is used in this paper:

$$\beta = \frac{-184.05}{1 + e^{(\phi+0.56468)/0.09425}} + 0.99494 \tag{5}$$

For consolidated sediment, the equation by Raymer and others (1980), which is written in the following form by Krief and others (1990), can be used.

$$\beta = 1 - (1-\phi)^{3.8} \tag{6}$$

Because the Biot coefficient shown in equations 5 and 6 is independent of differential pressure, it is not suitable to model velocities with respect to differential pressure. However, the dependence of velocity on differential pressure can be incorporated by using a variable n as a function of differential pressure.

Parameters *G* and *n*

In Lee (2003), it is demonstrated that the scale G depends on clay content in sediments and is given by the following formula:

$$G = 0.9552 + 0.044 e^{-C_v/0.06714} \tag{7}$$

where

C_v is the clay-volume content.

Equation 7 indicates that G is equal to 1 for clean sands. Without explicit use of C_v, clean sandstones are assumed in this investigation.

The exponent n is the most important parameter in BGTL and is proposed by the following function:

$$n = [10^{(0.426 - 0.235 Log_{10} p)}]/m \tag{8}$$

where

p is differential pressure (difference between pore pressure and overburden pressure) in MPa, and

m is a constant to be determined.

Equation 8 is derived from Prasad's data (2002) measured at differential pressure between 0.001 and 50 MPa with the Biot coefficient given in equation 5.

Constant *m*

To a first-order approximation, the constant *m* appears to depend on the degree of consolidation of sediments, and *m* becomes larger as the degree of consolidation/compaction increases. As can be seen from equation 8, as *m* increases, *n* decreases. As indicated in Lee (2003), elastic velocities mainly depend on the exponent *n* and increase as *n* decreases or the degree of consolidation increases. Also, as *n* increases or *m* decreases, V_p/V_s increases.

Figure 1 shows the porosity variation with respect to differential pressure and constant *m*. Porosity decreases as depth or differential pressure increases by packing, compaction and cementation (Schön, 1996). In this paper, in order to quantify the constant *m*, the degree of compaction is defined as the rate of porosity change due to elastic rebound with respect to differential pressure ($\partial\phi/\partial p$). Generally, the magnitude of $\partial\phi/\partial p$ is related to the degree of consolidation as well as the degree of compaction, making it difficult to differentiate one from the other. Therefore, in this paper, the degree of consolidation is used interchangeably with the degree of compaction.

Porosity reduction by compaction is shown in figure 1*A* as solid lines; sandstone and shale lines are from Sclater and Christie (1985). The shale compaction curve is given by $\phi = 0.803e^{-5.1d/10000}$, and the sandstone compaction curve is given by $\phi = 0.49e^{-2.7d/10000}$, where *d* is depth in meters. Porosity change with respect to depth or differential pressure due to compaction is large. However, porosity changes with respect to differential pressure for samples examined by Prasad (2002), Domenico (1977), and Han and others (1986) are much smaller than that shown on the compaction curves because compaction is predominantly an inelastic process and only a small amount of elastic rebound occurs when dif-

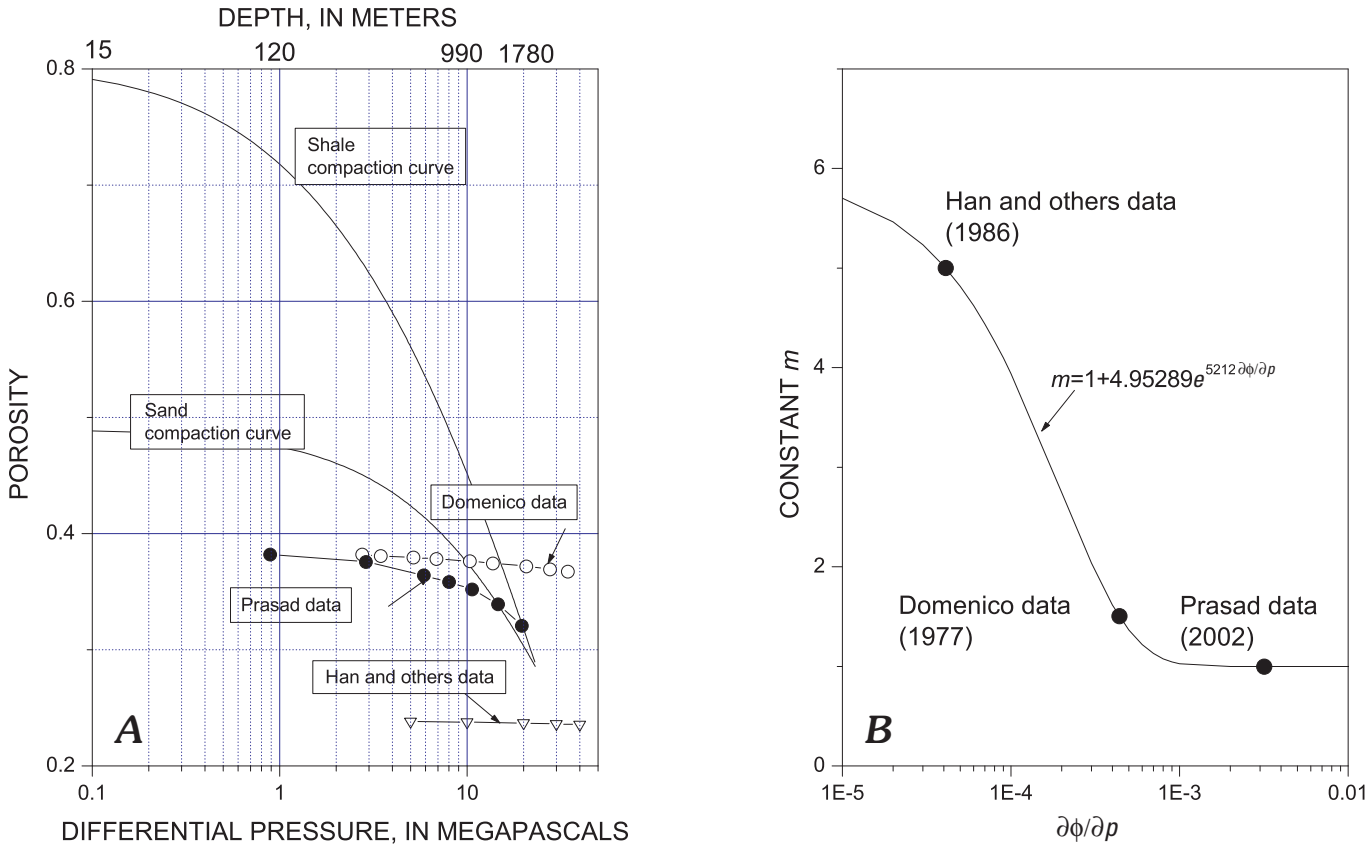

Figure 1. Graph showing porosity reduction with respect to differential pressure and variation of constant *m*. *A*, Porosity versus differential pressure for measured data by Domenico (1977), Han and others (1986), and Prasad (2002). Sand and shale compaction curves are calculated from Sclater and Christie (1980). *B*, Constant *m* with the rate of porosity reduction with respect to differential pressure. Average rate of porosity change with respect to differential pressure for Domenico, Han and others (only five clean sandstones), and Prasad data, shown as large solid circles, and a least-squares fitting curve are shown.

ferential pressure acting on a formation is reduced (unloading) (Bowers, 2002). An interesting point shown in figure 1*A* is that the rate of porosity decrease with respect to differential pressure is different among samples by Prasad, Domenico, and Han and others. The average $\partial\phi/\partial p$ values for data by Prasad, Domenico, and Han and others are -3.2×10^{-3}/MPa, -4.4×10^{-4}/MPa, and -4.1×10^{-5}/MPa, respectively. (The rate for data by Han and others data is the average of five clean sand samples for a differential pressure range between 10 and 40 MPa). As shown later, velocities or velocity ratios computed by BGTL using equation 8 with $m = 1$, $m = 1.5$, and $m = 5$ agree well with those of Prasad, Domenico, and Han and others. Based on the above $\partial\phi/\partial p$ and m, the following equation for m is derived by a least-squares method and is shown in figure 1*B*. The equation is:

$$m = 1.0 + 4.95289 e^{5212\,\partial\phi/\partial p} \quad (9)$$

Equation 9 indicates that, as $\partial\phi/\partial p$ approaches zero, m approaches about 6, and, as $\partial\phi/\partial p$ approaches a large negative number, m approaches 1. In deriving equation 9, only three input points by Domenico, Han and others, and Prasad are used and the least-squares fitting to the exponential function is exact. Therefore, it is not known whether equation 9 is appropriate for other values of $\partial\phi/\partial p$. Note that $\partial\phi/\partial p$ in equation 9 applies only to porosity changes owing to elastic rebound (unloading process). Therefore, in general, equation 9 may not be used for the sand or shale compaction curve. In practice, $\partial\phi/\partial p$ is rarely known; thus, a direct application of equation 9 is limited. Measured data suggest that $m \approx 4$–6 is appropriate for consolidated sediments at differential pressures above about 30 MPa and $m \approx 1$–2 is suitable for unconsolidated sediments at differential pressures of about 10 MPa or less.

Analysis and Modeling

The elastic constants used in this study are given in table 1.

Velocity Ratio with Respect to Differential Pressure

Velocities in sediments depend primarily on differential pressure and porosity. For a given sediment, as differential pressure increases, porosity decreases as shown in figure 1. In order to accurately predict elastic velocities with respect to differential pressure, porosity changes owing to differential pressure should be incorporated, particularly for unconsolidated sediments. The general behavior of porosity variation with respect to differential pressure is not accurately known. Therefore, in this paper, data in table 4 by Prasad (2002) are used to derive a relationship between porosity and differential pressure; this relationship is given as follows:

$$\phi = 0.38452 - 0.00319p \quad (10)$$

The porosity range for Prasad's data is between 0. 382 at p = 0.89 MPa and 0.321 at p =19.67 MPa (actually Prasad, 2002, provided density instead of porosity—porosity is calculated assuming a matrix density of 2.65 g/cm^3 and a fluid density of 1.0 g/cm^3). Therefore, all the calculated results are accurate for these porosity and differential pressure ranges.

Figure 2 shows measured and computed velocity ratios with respect to differential pressure. Circles are measured ratios complied by Prasad (2002). The measured velocity ratio appears to be a linear function of pressure in log-log scale, and Prasad derived a least-squares fitting curve, which is given by $V_p/V_s = 5.6014p^{-0.2742}$. As indicated in figure 2, the predicted ratio by BGTL using n given by equation 9 with $m = 1$ is close to the measured ratio at a differential pressure greater than about 0.5 MPa, but the computed ratio is much larger than that predicted by the linear function for a differential pressure of less than about 0.5 MPa. The dashed line is the least-squares fitting curve for the data analyzed by Huffman and Castagna (2001) and agrees well with the prediction of BGTL with m = 1.3 in equation 9 for a differential pressure greater than about 0.2 MPa. As differential pressure decreases, the difference between the two curves increases.

Table 1. Elastic constants used in this paper.

Elastic constant	Value used	Source
Shear modulus of quartz	44 Gpa	Carmichael (1989)
Bulk modulus of quartz	38 Gpa	Carmichael (1989)
Shear modulus of clay	6.85 Gpa	Helgerud and others (1999)
Bulk modulus of clay	20.9 Gpa	Helgerud and others (1999)
Bulk modulus of water	2.29 Gpa	
Density of quartz	2.65 g/cm^3	Helgerud and others (1999)
Density of clay	2.58 g/cm^3	Helgerud and others (1999)
Density of water	1.0 g/cm^3	

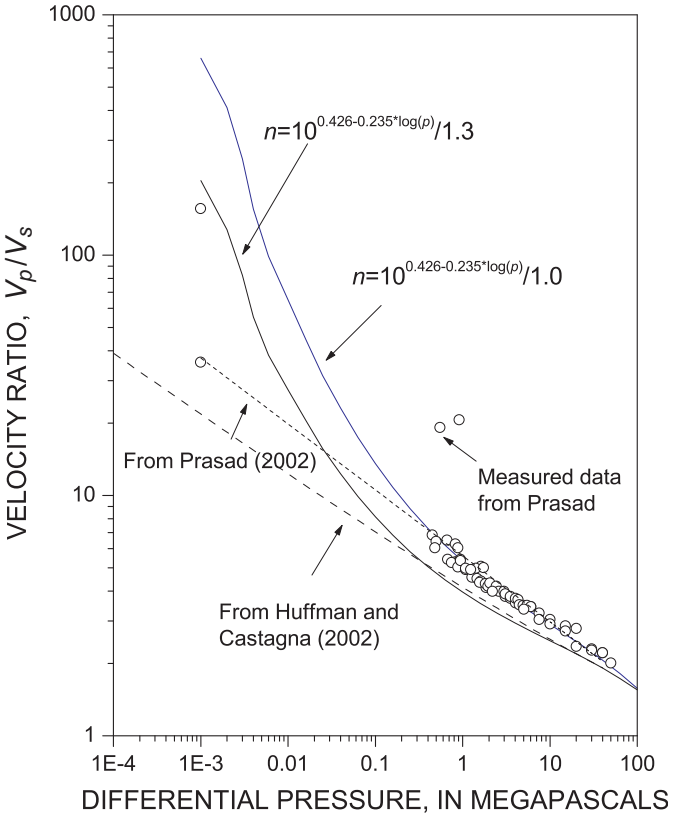

Figure 2. Graph showing computed and measured velocity ratio (V_p/V_s) with respect to differential pressure. Open circles are measured V_p/V_s from data complied by Prasad (2002, table 3); the dotted line is a least-squares fitting curve to the measured data by Prasad; and the dashed line is a least-squares fitting curve to the measured data by Huffman and Castagna (2001).

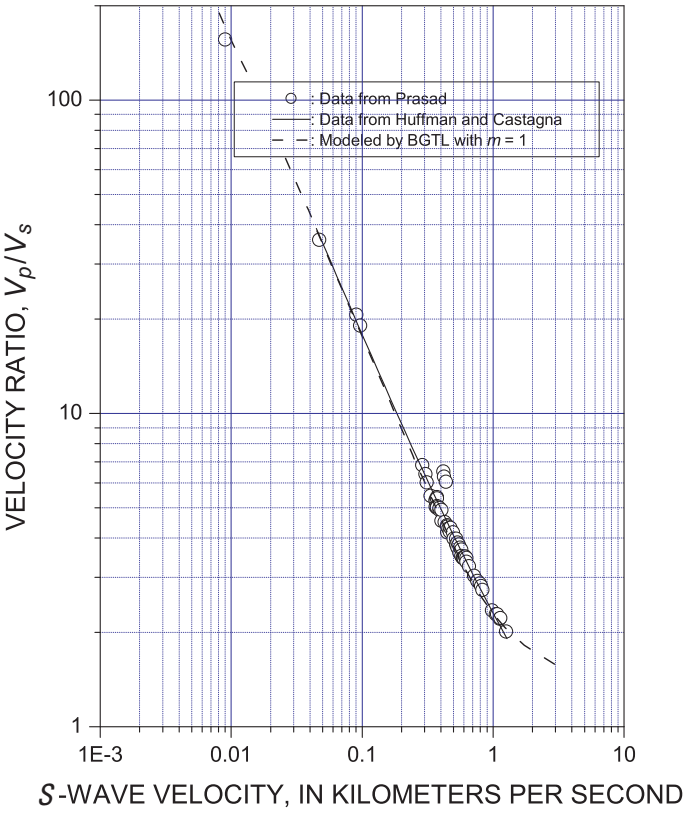

Figure 3. Measured and calculated velocity ratios with respect to *S*-wave velocity. Open circles represent data in table 3 from Prasad (2002); the solid line is the least-squares fit to the measured data by Huffman and Castagna (2001); and the dashed line is the calculated velocity ratio from Biot-Gassmann theory by Lee (BGTL).

Velocity Ratio with Respect to *S*-Wave Velocity

Differential pressure, clay content, porosity, degree of consolidation, and other factors affect V_p/V_s and velocities in the sediment. Figure 3 shows V_p/V_s with respect to *S*-wave velocity. BGTL with a variable *n* computed from equation 8 fits most of the measured data complied by Prasad (2002) and the least-squares fitting curve by Huffman and Castagna (2002). The trend of V_p/V_s with respect to differential pressure for data compiled by Prasad (2002) shows a different trend compared to that by Huffman and Castagna (2001), whereas the trend with respect to *S*-wave velocity is the same. This implies that the best predictor of V_p/V_s for sediments including SWF sand or overpressured sand is using *S*-wave velocity as an independent variable. In this way, variability of V_p/V_s associated with differential pressure, porosity, and degree of consolidation is reduced.

Velocity with Respect to Porosity and Differential Pressure

The predicted velocity ratio (V_p/V_s) in the previous section indicates that BGTL is accurate for differential pressures greater than about 0.1–0.2 MPa. However, the accuracy of the velocity ratio predicted from the BGTL does not imply that the BGTL is accurate for the velocities themselves. In order to examine the accuracy of BGTL, elastic velocities are computed with respect to porosity and differential pressure, and are shown in figure 4.

Figure 4*A* shows velocities with respect to porosity computed from equation 10. Open and solid circles represent measured velocities for differential pressures between 0.89 and 19.67 MPa (table 4 from Prasad, 2002). Overall, velocities predicted by BGTL are slightly lower than measured velocities, but BGTL accurately predicts the trend between

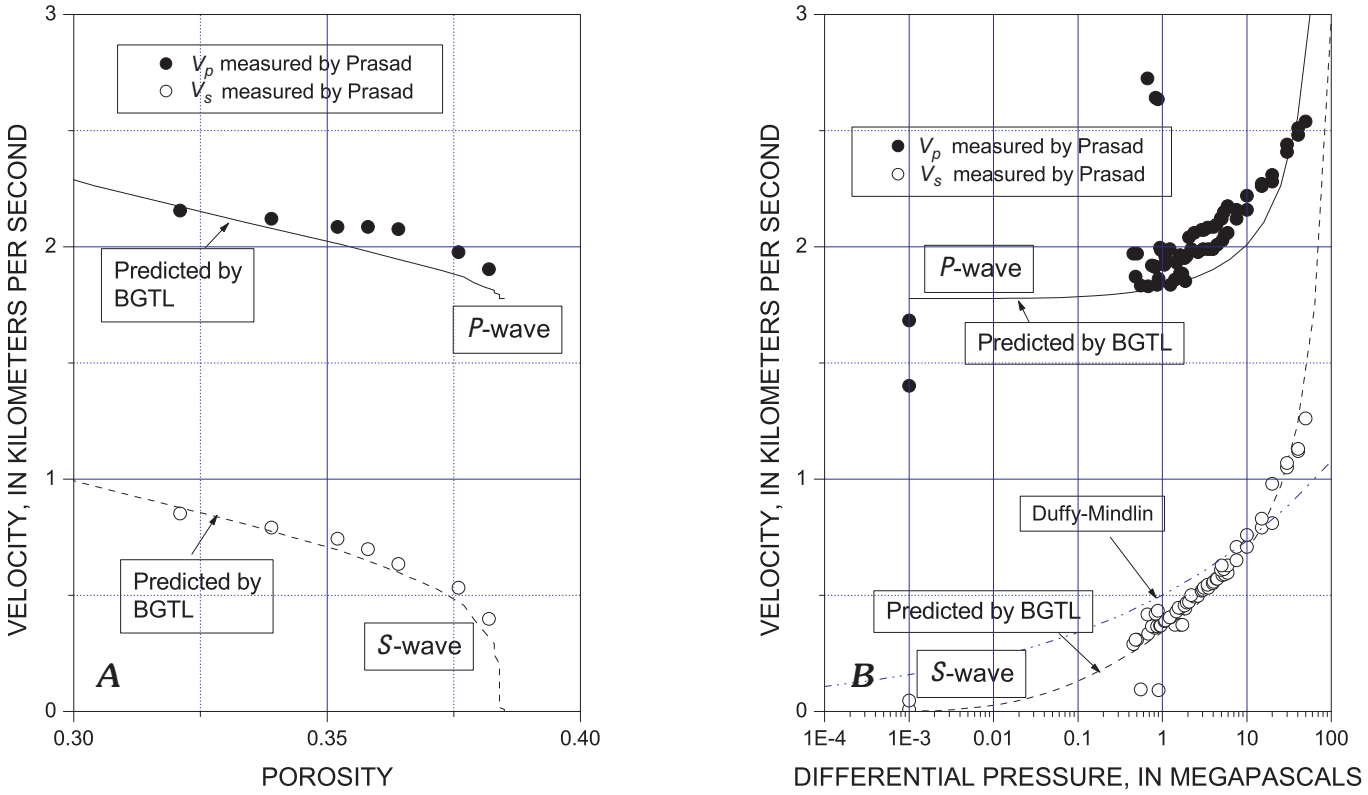

Figure 4. Calculated velocities by Biot-Gassmann theory by Lee (BGTL), Duffy-Mindlin theory (1957), and measured velocities by Prasad (2002) with respect to porosity and differential pressure. Measured velocities are from tables 3 and 4 in Prasad. *A*, Velocity versus porosity for measured data in table 4 of Prasad (2002). *B*, Velocity versus differential pressure for measured data in table 3 of Prasad (2002). The dependence of differential pressure on *S*-wave velocity from Duffy-Mindlin theory is a power of 1/6 ($p^{1/6}$), whereas it is $p^{0.337}$ based on a least-squares fitting to the measured data.

velocity and porosity. Figure 4*B* shows computed velocities with all measured velocities (table 3 from Prasad, 2002). As in figure 4*A*, predicted velocities are slightly lower than measured velocities and BGTL predicts *S*-wave velocities more accurately than *P*-wave velocities. Note that predicted *S*-wave velocities near $p = 0.001$ MPa are close to measured *S*-wave velocities.

Prediction of Pore Pressure

It is generally recognized that pore pressure can be detected prior to drilling using velocity analysis because overpressured intervals show significantly reduced interval velocities and large V_p/V_s. From AVO analysis (Huffman and Castagna, 2001), full waveform inversion (Dutta, 2002), or multicomponent seismic data (Sayers and others, 2002), velocities and V_p/V_s can be estimated from seismic data. If velocity ratios or *S*-wave velocities are available, differential pressures can be estimated from figure 5.

Figure 5 shows calculated V_p/V_s, *S*-wave velocity, and differential pressure from BGTL with $m = 1$ and $m = 1.3$ using porosity given by equation 10. Figure 5 is a combination of figures 3 and 4 using *S*-wave velocity as an independent variable. As shown in figure 5, the predicted V_p/V_s by BGTL is insensitive to the degree of compaction (compare solid and dotted lines of V_p/V_s), but differential pressure strongly depends on the degree of compaction. Open circles in figure 5 represent the measured V_p/V_s, and solid circles represent measured differential pressures compiled by Prasad (2002). Because V_p/V_s with respect to *S*-wave velocity is insensitive to different data sets, as opposed to V_p/V_s with respect to differential pressure, it has the advantage of using *S*-wave velocity as a common variable to relate V_p/V_s to differential pressure. Let us assume that the measured V_p/V_s is 8. Figure 5 indicates that $V_p/V_s = 8$ corresponds to *S*-wave velocity of about 0.2 km/s and differential pressure is about 0.3 MPa if $m = 1$ is applicable, or $p = 0.1$ MPa if $m = 1.3$ is applicable. Either V_p/V_s or *S*-wave velocity can be used to estimate differential pressure.

The *P*-wave velocity also can be used to predict overpres-

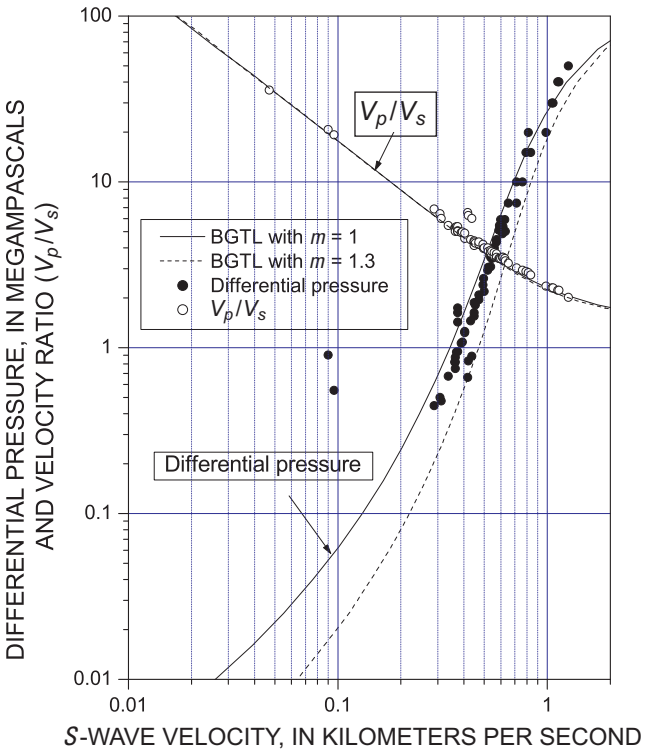

Figure 5. Graph showing relationship among differential pressure, V_p/V_s, and the *S*-wave velocity. Open and solid circles are measured V_p/V_s and differential pressure, respectively, for data complied by Prasad (2002).

sure. However, as indicated in figure 4*B*, the *P*-wave velocity is almost constant for differential pressures of less than about 1 MPa. Therefore, the *P*-wave velocity is not an accurate indicator at low differential pressures.

Discussion

Velocity Ratio and Differential Pressure

Results shown on figure 2 indicate that BGTL accurately predicts the V_p/V_s ratio with respect to differential pressure for data compiled by Prasad (2002) except for four anomalous points. Two anomalous points near p = 0.001 MPa are measured ratios for near-surface marine sediments of the continental slope of the Bearing Sea by Ayers and Theilen (1999). Prasad's linear equation fits one of the anomalous points, whereas the predicted ratio by BGTL is much larger than the measured ratio. Because there are no other measurements between p = 0.5 MPa and p = 0.001 MPa, it is difficult to assess the accuracy of BGTL or the linear function of Prasad for differential pressures less than about 0.5 MPa.

Higher V_p/V_s ratios—predicted from BGTL for p less than about 0.2 MPa—come from the fact that V_p is almost constant for differential pressures between 1 and 0.001 MPa, while V_s decreases monotonically to zero (fig. 4*B*). This kind of behavior of *P*- and *S*-wave velocity is expected for water-saturated sediments. Therefore, the prediction of BGTL for differential pressures less than 2 MPa appears to be reasonable. However, the accuracy of BGTL for this low differential pressure cannot be established until more data are available in the low-pressure range.

Both Prasad (2002) and Huffman and Castagna (2001) demonstrate a linear relationship between log (V_p/V_s) and log (p), although Prasad's equation predicts a higher V_p/V_s at a given differential pressure. Huffman and Castagna (2001) suspected that this difference is due to higher porosities in Prasad's samples. Usually, higher porosity samples yield higher V_p/V_s ratios, so this conjecture is reasonable. However, figure 2 indicates that BGTL with m = 1.3 instead of m = 1, which is good for the Prasad data, predicts accurate V_p/V_s values for the Huffman and Castagna data, although the same porosities (equation 9) are used. As mentioned in Lee (2003), the constant m is introduced in order to incorporate the degree of compaction. Therefore, another interpretation of Huffman and Castagna data is that the degree of compaction of samples used by Prasad is less than that used by Huffman and Castagna.

The interpretation that lower V_p/V_s values at a given differential pressure implies a more consolidated nature of sediment may be explained using figure 6, where the Domenico (1977) and Prasad (2002) data are shown. The data set used to derive a relationship between V_p/V_s and differential pressure by Huffman and Castagna (2001) included the data measured by Domenico (1977). Although porosities at low differential pressure are similar, the rate of porosity decrease with respect to differential pressure in the Prasad data is much higher than that of the Domenico data, as previously mentioned. In other words, the Prasad sample is softer or easier to compact than the Domenico sample.

Figure 6 shows measured and calculated V_p/V_s with respect to differential pressure for sediments with differing porosities. Clearly, assuming the same value of m, calculated V_p/V_s values of higher porosity sediments is larger than those of lower porosity sediments (compare the solid and dashed lines). This implies that, for sediments having a similar degree of consolidation/compaction, the higher the porosity, the larger V_p/V_s will be. Also note that V_p/V_s of sediment having a porosity of 30 percent with m = 1 (dot-triangle-dot) is almost the same as that of sediments having a porosity of 40 percent with m = 1.5 (dashed line). This suggests that, as far as V_p/V_s is concerned, it is difficult to determine whether the increase of V_p/V_s is owing to an increase of porosity or to a decrease of consolidation/compaction.

Figure 6 indicates that V_p/V_s for Domenico's data (open circles) is less than that for Prasad's data (solid circles), even

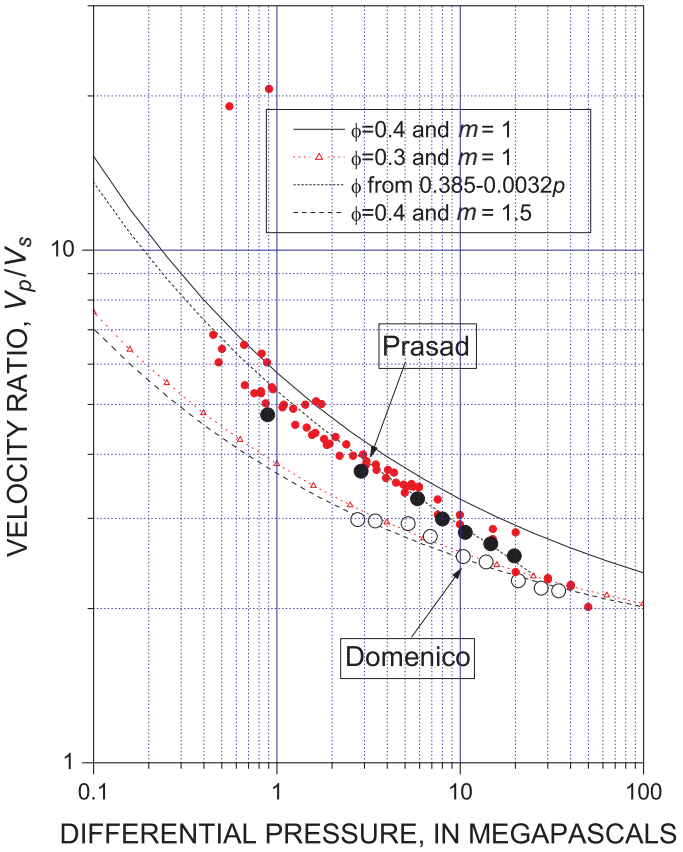

Figure 6. Graph showing V_p/V with respect to differential pressure. Measured data are shown as open circles (Domenico, 1977) and as solid circles (Prasad, 2002). Light small solid circles are for all samples by Prasad (his table 3) and large dark solid circles are for a subset of Prasad data (his table 4). Modeled velocity ratios are derived from BGTL with $m = 1$ and $m = 1.5$ with various porosities.

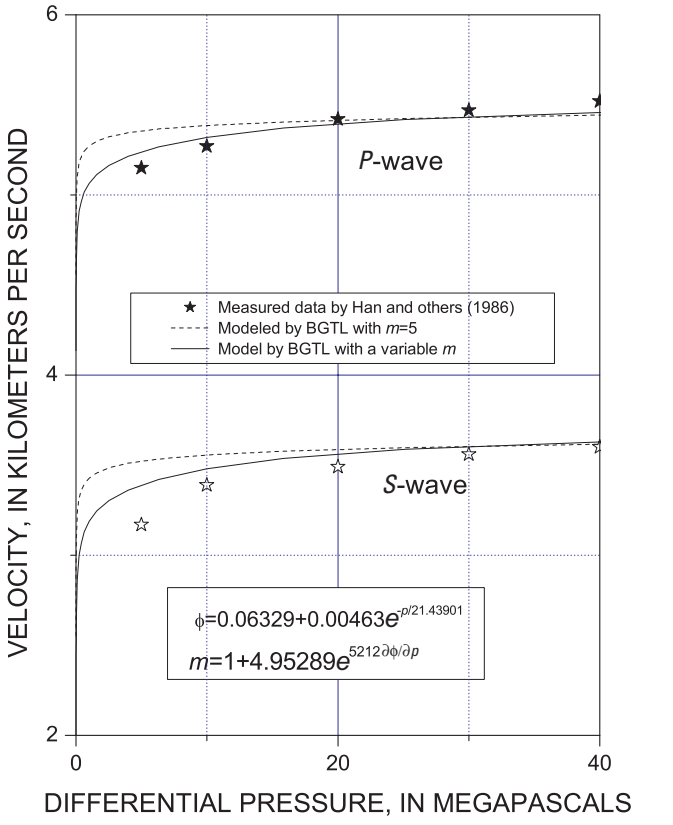

Figure 7. Measured and computed velocities from BGTL with respect to differential pressure are shown. Measured velocities are for a clean sandstone having a porosity of 0.0670 at 5 MPa by Han and others (1986). Dotted lines represent predicted velocities using the Biot coefficient shown in equation 6 with a constant $m = 5$ and solid lines are with a variable m calculated from equation 9 with $\phi = 0.06329 + 0.00463e^{-p/21.439}$.

though porosity values in Domenico's data are higher than those in Prasad's data, as shown in figure 1*A*. The measured V_p/V_s shown in figure 6 (large solid circles are data from table 4 and small solid circles are data from table 3 in Prasad, 2002) indicates that the discrepancy between Prasad's and Domenico's data increases as differential pressure decreases or the porosity of Prasad's samples approach those of Domenico's (1977). Therefore, figures 1 and 7 suggest that the difference in V_p/V_s between the Prasad and the Huffman and Castagna data may come from the difference in the degree of compaction, not from the difference in porosity as suggested by Huffman and Castagna (2001).

Differential Pressure and *S*-Wave Velocity

In order to incorporate the effect of differential pressure on elastic velocities, a contact model based on the Hertz theory has been used. Duffy and Mindlin (1957) applied the Hertz theory to face-centered sphere space—most analogous to a clean, well-sorted, deep-marine, unconsolidated sand—and showed that the velocity is proportional to 1/6 power of differential pressure. The prediction of the Duffy-Mindlin theory is shown in figure 4*B* as dash-dot-dot. The least-squares fitting of *S*-wave velocities with respect to differential pressure is given by $V_s = p^{0.337}/0.332$. The theoretical prediction of the effect of differential pressure on velocity based on the contact theory is about one-half of the observed effect. This observation is different from that by Merkel and others (2001), who demonstrated that the reservoir rocks, massive turbidites in the Gulf of Mexico, behave in accordance with the Duffy-Mindlin theory.

In the BGTL formulation, the effect of differential pressure on velocity is incorporated by using the pressure-dependent exponent n. As indicated in equation 8, n is a function of differential pressure and m. As shown in previous sections, the data compiled by Prasad (2002) fit the prediction of the BGTL with $m = 1.0$ and with $m = 1.3$ for the Domenico data (1977).

The exponent of 1/6, predicted by Duffy-Mindlin theory, is approximately achieved by using BGTL with $m = 4$. Therefore, the degree of consolidation of reservoir rocks analyzed by Merkel and others (2001) may be much higher than that analyzed in this paper.

Clay Effect on Velocity Ratio

Contribution of clay on V_p/V_s at low differential pressures is not analyzed in this paper because of the lack of available data. However, a brief and qualitative discussion is included in order to show a strange V_p/V_s of shaly sand. Huffman and Castagna (2002) indicate that V_p/V_s of sand containing 8 percent clay by weight is lower than that of clean sand—they interpreted that small amounts of clay act to bind loose sand grains, thereby decreasing V_p/V_s at a given pressure. Usually, clay in consolidated sand decreases *S*-wave velocity more than *P*-wave velocity, so clay increases the V_p/V_s of the sediment (Blangy and others, 1993; Lee, 2003). This is opposite to the observation by Huffman and Castagna (2002). Clay in sediments affects the rate of porosity reduction with respect to differential pressure as well as porosity itself; thus, both effects contribute to the variation of V_p/V_s. Therefore, without detailed knowledge about the porosity and porosity reduction of shaly sand, it is not conclusive whether clay increases or decreases V_p/V_s of unconsolidated sediments with respect to differential pressure.

BGTL Parameter *m*

As shown in figure 5, determination of an accurate *m* is important to reduce the uncertainty of the estimated differential pressure. As mentioned previously, *m* appears to depend on $\partial\phi/\partial p$, and Prasad (2002) and Domenico (1977) data suggest that the proposed equation 9 for *m* is adequate. Figure 7 shows velocity versus differential pressure for a clean sandstone sample having a porosity of 0.067 at 5 MPa from Han and others (1986). Predicted velocities using BGTL with $m = 5$ agree well with the measured velocities for a differential pressure above 20 MPa, but velocities are higher than measured velocity at low differential pressures. This is caused by using a constant *m* irrespective of $\partial\phi/\partial p$. By fitting the porosity with respect to differential pressure as $\phi = 0.06329 + 0.00463e^{-p/21.43901}$, a variable *m* using equation 9 is attempted to examine whether the proposed equation for *m* is really a function of $\partial\phi/\partial p$. Figure 7 shows the predicted velocities using a variable *m*, e.g., $m = 5.11$ at $p = 40$ MPa and $m = 3.44$ at $p = 10$ MPa, as solid lines. Predicted velocities with variable *m* are still higher than measured velocities at low differential pressure, but the predicted rate of velocity change with respect to differential pressure agrees reasonably well with the measured rate.

The above analysis supports the idea that the constant *m* is a function of $\partial\phi/\partial p$. However, because $\partial\phi/\partial p$ is rarely known in practice and because equation 10 for *m* is based on only three samples, it is difficult to use equation 10 directly. A proper choice of *n* and *m* is important to use BGTL effectively, and equations 8 and 9 provide general guidelines for the estimation of *n* and *m*.

Conclusions

Biot-Gassmann theory by Lee (BGTL) accurately predicts the velocity ratio (V_p/V_s) with respect to differential pressure by using a variable exponent in the form of $n = [10^{a+b\log(p)}]/m$. Pore pressure or differential pressure can be estimated from V_p/V_s or the *S*-wave velocity by utilizing the fact that the V_p/V_s ratio with respect to the *S*-wave velocity depends strongly on differential pressure and is less sensitive to porosity and clay content. A proper choice of the constant *m* is important to reduce the uncertainty of the estimated differential pressure. As *m* increases, V_p/V_s decreases at a given differential pressure and appears to depend strongly on the rate of porosity reduction with respect to differential pressure.

For differential pressures greater than about 0.5 MPa , BGTL with $m = 1$ accurately predicts the V_p/V_s ratio for measured data complied by Prasad (2002), and BGTL with $m = 1.3$ is satisfactory for data analyzed by Huffman and Castagna (2001). Whether or not the prediction of V_p/V_s by BGTL is more accurate than that predicted by empirical relationships at low differential pressures is not clear because of the paucity of measured data at low differential pressure (less than 0.5 MPa).

To use BGTL effectively, a proper choice of the exponent *n* is important, which can be regarded as a free parameter to fit observations. However, this study shows that general guidelines based on differential pressure and the degree of compaction work well for a variety of data sets.

References

Ayers, A, and Theilen, F., 1999, Relationship between P- and S-wave velocities and geological properties of near-surface sediments of the continental slope of the Barents Sea: Geophysical Prospecting, v. 47, p. 431–441.

Biot, M.A., 1956, Theory of propagation of elastic waves in a fluid saturated porous solid. I. Low-frequency range and II. High-frequency range: Journal of Acoustical Society of America, v. 28, p. 161–191.

Blangy, J.P., Strandenes, S., Moos, D., and Nur, A., 1993, Ultrasonic velocities in sands—Revisited: Geophysics, v. 58, p. 344–356.

Bowers, G.L., 2002, Detecting high overpressure: The Leading Edge, v. 21, p. 174–177.

Bruce, B., Borel, R., and Bowers, G., 2002, Well planning for SWF and overpressure at the Kestrel well: The Leading Edge, v. 21, p. 669–671.

Carmichael, R.S., 1989, Practical handbook of physical properties of rocks and minerals: CRC Press, 741 p.

Domenico, S.N., 1977, Elastic properties of unconsolidated porous sand reservoirs: Geophysics, v. 42, p. 1339–1368.

Duffy, J., and Mindlin, R.D., 1957, Stress-strain relations and vibrations of a granular medium: Journal of Applied Mechanics, v. 24, p. 585–593.

Dutta, N.C., 2002, Geopressure prediction using seismic data: Current status and the road ahead: Geophysics, v. 67, p. 2012–2041.

Han, D, Nur, A., and Morgan D., 1986, Effects of porosity and clay content on wave velocities in sandstones: Geophysics, v. 51, p. 2093–2107.

Helgerud, M.B., Dvorkin, J., Nur, A., Sakai, A., and Collett, T., 1999, Elastic-wave velocity in marine sediments with gas hydrates: Effective medium modeling: Geophysical Research Letters, v. 26, p. 2021–2024.

Huffman, A.R., and Castagna, J.P., 2001, The petrophysical basis for shallow-water flow prediction using multicomponent seismic data: The Leading Edge, v. 20, p. 1030–1035, 1052.

Gassmann, F., 1951, Elasticity of porous media: Vierteljahrsschr der Naturforschenden Gesselschaft, v. 96, p. 1–23.

Krief, M., Garta, J., Stellingwerff, J., and Ventre, J., 1990, A petrophysical interpretation using the velocities of P and S waves (full-waveform sonic): The Log Analyst, v. 31, p. 355–369.

Lee, M.W., 2002, Biot-Gassmann theory for velocities of gas-hydrate-bearing sediments: Geophysics, v. 67, p. 1711–1719.

Lee, M.W., 2003, Velocity ratio and its application to predicting velocities: U.S. Geological Survey Bulletin 2197, 15 p. [http://geology.cr.usgs.gov/pub/bulletins/b2197].

Mallick S., and Dutta, N.C., 2002, Shallow water flow prediction using prestack waveform inversion of conventional 3D seismic data and rock modeling: The Leading Edge, v. 21, p. 675–680.

Merkel, R.H., Barree, R.D., and Towle, G., 2001, Seismic response of Gulf of Mexico reservoir rocks with variations in pressure and water saturations: The Leading Edge, v. 20, p. 290–299.

Ostermeier, R.M., Pelletier, J.H., Winkler, C.D., Nicholson, J.W., Rambow, F.H., and Cowan, K.M., 2002, Dealing with shallow-water flow in the deepwater Gulf of Mexico: The Leading Edge, v. 21, p. 660–668.

Prasad, M., 2002, Acoustic measurements in unconsolidated sands at low effective pressure and overpressure detection: Geophysics, v. 67, p. 405–412.

Raymer, L.L., Hunt, E.R., and Gardner, J.S., 1980, An improved sonic transit time to porosity transform: 21st Annual Society of Professional Well Log Analysts Logging Symposium Transactions, Paper P.

Sayers, C.M., Woodward, M.J., and Bartman, R.C., 2001, Predrill pore-pressure prediction using 4-C seismic data: The Leading Edge, v. 20, p. 1056–1059.

Sayers, C.M., Woodward, M.J., and Bartman, R.C., 2002, Seismic pore-pressure prediction using reflection tomography and 4-C seismic data: The Leading Edge, v. 21, p.188–192.

Sclater, J.C., and Christie, P.A.F., 1980, Continental stretching: An explanation of the post mid Cretaceous subsidence of the central North Sea basin: Journal of Geophysical Research, v. 85, p. 3711–3739.

Schön, J.H., 1996, Physical properties of rocks: Pergamon, 583 p.

Zimmer, M., Prasad, M., and Mavko, G., 2002, Pressure and porosity influences on V_p-V_s ratios in unconsolidated sands: The Leading Edge, v. 21, p. 178–183.

Manuscript approved for publication August 28, 2003
Published in the Central Region, Denver, Colorado
Editing, layout, photocomposition—Richard W. Scott, Jr.
Graphics by the author